A Beaker without Walls: Formation of Deeply Supercooled Binary Liquid Solutions of Alcohols from Nanoscale Amorphous Solid Films

Patrick Ayotte, R. Scott Smith, Glenn Teeter, Zdenek Dohnálek, Gregory A. Kimmel, and Bruce D. Kay*

Environmental Molecular Sciences Laboratory, Pacific Northwest National Laboratory, P.O. Box 999, Mail Stop K8-88, Richland, Washington 99352

(Received 27 November 2001; published 3 June 2002)

Layered nanoscale amorphous solid films of methanol and ethanol undergo complete intermixing prior to the onset of measurable desorption at 120 K. This intermixing precedes and inhibits crystallization. Subsequent desorption of the film is described quantitatively by a kinetic model describing evaporation from a continuously mixed ideal binary liquid solution. This occurs at temperatures below the melting point of the binary mixture, indicating ideal behavior for the supercooled liquid solution. This approach provides a new method for preparing and examining deeply supercooled solutions.

DOI: 10.1103/PhysRevLett.88.245505 PACS numbers: 61.25.Em, 66.30.Pa, 68.15.+e, 82.60.Lf

Supercooled liquids are metastable and their lifetimes are dictated by the kinetics for crystallization [1]. Traditional experimental studies have used a variety of methods to suppress crystallization while cooling from the liquid phase [2]. An alternate approach is to heat an amorphous solid above its glass transition temperature, T_g, whereupon it transforms into a deeply supercooled liquid prior to crystallization [3,4]. We demonstrate that compositionally tailored nanoscale films of glassy methanol and ethanol exhibit complete diffusive intermixing and suppressed crystallization when heated above T_g. Furthermore, the resulting containerless liquids evaporate as continuously mixed ideal binary solutions while retaining their solidlike macroscopic shapes.

Nanoscale amorphous binary films of methanol (M) and ethanol (E) were grown at 20 K on a Pt(111) single crystal in an ultrahigh vacuum chamber using molecular beam techniques. The molecular beam allows for precise calibration of the deposited amount. At this temperature and at normal incidence, the vapor-deposited material forms a dense amorphous solid [5]. Composite films having a diameter ~6 mm were grown by sequential dosing of methanol and ethanol. Experiments where methanol was deposited on top of ethanol (M/E) and where ethanol was deposited on top of methanol (E/M) were conducted. The composite films were then heated and the desorption of methanol and ethanol was measured mass spectrometrically. Concurrent evaluation of the condensed phase chemical composition and physical state (amorphous versus crystalline) was performed using reflection-absorption infrared spectroscopy (RAIRS).

Comparison of the desorption traces from composite films grown with alternate dosing sequences (i.e., M/E versus E/M) yields information about the extent of diffusive intermixing. In the absence of intermixing, desorption from these composite films would result in the species deposited on top evaporating first and impeding the evaporation from the species deposited underneath [6]. Complete intermixing would result in desorption traces independent of the initial dose order. Incomplete intermixing results in complex desorption traces as described previously [3]. The results from thermal desorption experiments on composite methanol-ethanol films were independent of dose order for films as thick as 300 total layers (~100 nm). Furthermore, initially layered binary amorphous films displayed identical results to those from samples that were grown with molecular beams made from premixed vapors. These observations indicate that initially layered amorphous films have completely intermixed prior to the onset of measurable methanol desorption ($T \sim 120$ K).

Given the observed intermixing, it is possible to estimate a lower limit for the diffusivity of the binary films using the relation $D \sim L^2/t$. Mixing occurs over a distance of 100 nm in approximately 10 s requiring diffusivities in excess of 10^{-11} cm^2/s at $T \sim 120$ K. This diffusivity is consistent with extrapolations of the pure liquid diffusivities to this temperature and about a millionfold smaller than their diffusivities at room temperature [7]. This finding indicates that the individual amorphous solid constituents of the sample intermix and exhibit liquidlike behavior on the nanoscale while the sample maintains its macroscopic solidlike shape.

Previous calorimetric [8,9] and infrared [10] studies have demonstrated that pure amorphous methanol and ethanol crystallize upon heating above their respective glass transition temperatures of 103 and 97 K. Figure 1 shows time sequences of the OH stretching region during isothermal annealing experiments for various films. Unlike the CH stretching region of the spectra, the OH stretching region is mostly independent of the sample's chemical composition and allows us to separate out spectral features arising from phase evolution. The bottom spectra [Fig. 1(A)] are for a 30-monolayer- (ML-) thick film of pure amorphous methanol annealed at 116 K. The first spectrum in the series (tail of arrow) displays the broad band characteristic of an amorphous solid [10], while subsequent spectra show the emergence of a narrower peak centered at 3310 cm^{-1}. A similar observation is

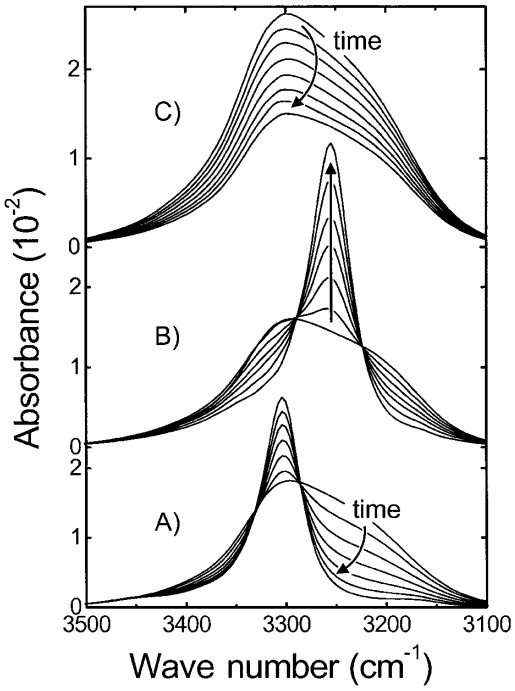

FIG. 1. Vibrational spectra of the OH stretching region during isothermal desorption experiments for (*A*) 30-ML-thick film of pure amorphous methanol annealed at 116 K, (*B*) 30-ML-thick film of pure amorphous ethanol annealed at 135 K, and (*C*) 60-ML-thick initially layered $x_M^0 = 0.5$ amorphous composite film of methanol and ethanol annealed at 135 K. The spectra illustrate the difference in behavior between the pure and mixed films (total time of 17 min, nonuniform time interval between spectra).

made during the annealing of a 30-ML-thick film of pure amorphous ethanol at 135 K [Fig. 1(*B*)]: the amorphous spectrum evolves into a relatively sharp peak centered at 3260 cm^{-1}. The last spectrum in each time sequence corresponds to the fully crystallized film [10]. Both sets of spectra display isosbestic points, indicating the conversion from the metastable amorphous to the stable crystalline phase.

In contrast to the pure films, the spectra for an initially layered binary amorphous film are observed to remain amorphouslike for the duration of the experiment at 135 K. Figure 1(*C*) displays the OH stretching region of a composite film of ethanol (30 ML) deposited on top of methanol (30 ML). As demonstrated below, the decrease in absorbance observed while annealing the binary film at 135 K results from the preferential evaporation of methanol from the mixture. The lack of crystallization in this composite film indicates that intermixing preceded and thereby inhibited the crystallization that occurs readily in pure amorphous methanol or ethanol. This behavior is consistent with the persistent supercooling observed in methanol-ethanol liquid mixtures [11]. This finding is also consistent with molecular dynamics simulations of binary mixtures of both Lennard-Jones [12] and hard sphere fluids [13]. These studies demonstrate that crystallization is inhibited due to the size difference between the two components of the binary supercooled solution. Additionally, we have recently demonstrated that extensive translational diffusion occurs in concert with the crystallization of amorphous solid water, a single component system [3].

The inhibition of crystallization in methanol-ethanol mixtures makes them well suited for studying deeply supercooled liquid solutions formed from nanoscale amorphous solids. The evaporation kinetics from these composite films provide a stringent test for whether or not these systems behave as homogeneous liquid solutions. Films with initial methanol mole fractions, x_M^0, between 0.15 and 1.00 were created at 20 K with a fixed 30 ML dose of methanol and various amounts of ethanol. In all cases, the results were independent of the initial dosing sequence (i.e., M/E versus E/M). Figure 2 displays the isothermal desorption of methanol from the pure (black line) and composite films (blue symbols) at 138 K. The constant desorption rate displayed by the pure methanol film is indicative of zero-order kinetics as expected for desorption from a pure substance. In contrast, the mixtures exhibit an apparently complicated temporal line shape that depends on x_M^0. At this temperature the total amount of ethanol in a given film remains nearly constant owing to its lower volatility. The conjugate ethanol spectra are omitted for clarity.

For the mixtures, the initial methanol desorption rate is observed to be proportional to x_M^0. This behavior is reminiscent of an ideal solution for which the partial vapor pressure of an individual component in a mixture is equal to the product of the vapor pressure of the pure substance

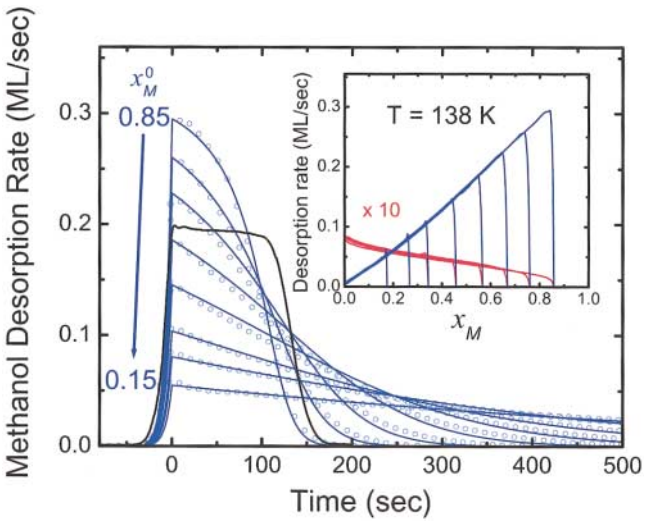

FIG. 2 (color). Isothermal (138 K) methanol desorption (heating rate of 0.6 K/s from 20 to 138 K) for a pure crystallized methanol film (black line) and amorphous binary films (open blue symbols) having initial methanol mole fractions $0.15 \leq x_M^0 \leq 0.85$. (For clarity only every thirtieth point is shown.) Ideal solution model simulations are shown as solid blue lines. Inset: methanol (blue) and ethanol (red) desorption rates plotted versus instantaneous methanol mole fraction, x_M.

and its mole fraction (i.e., Raoult's law) [14]. For an ideal solution, the partial vapor pressure is always less than the vapor pressure of the pure liquid. Interestingly, the isothermal desorption signal from the pure methanol film is smaller than that from composite films with $x_M^0 > 0.6$. This arises because the pure methanol film crystallized prior to reaching the isothermal desorption temperature (see Fig. 1). The desorption rate from crystalline methanol is lower than that from the metastable, supercooled liquid because of its lower free energy [15].

The solid blue lines in Fig. 2 are the result of simulations based on a kinetic model that treats evaporation from an ideal solution exhibiting rapid continuous mixing as the film evaporates. This mean-field model is based on two differential equations coupled through the methanol mole fraction. The time-dependent evaporation rates for methanol and ethanol are $dM/dt = x_M(t)k_M^o(T)$ and $dE/dt = [1 - x_M(t)]k_E^o(T)$, respectively. The methanol mole fraction is defined as $x_M(t) = M(t)/[M(t) + E(t)]$, where $M(t)$ and $E(t)$ are the amounts of methanol and ethanol remaining in the film at time t, respectively. We assume an Arrhenius form for the temperature-dependent evaporation rate $k_i^o(T) = \nu^i \exp(-E_a^i/RT)$ for the pure liquid component, i [16]. The coupled desorption equations are numerically integrated over the experimental temperature ramp. The quantitative agreement between the simulation and the experimental data indicates that the evaporation exhibits ideal behavior and that the samples continuously mix on a time scale fast relative to evaporation. To further demonstrate this, we plot in the inset of Fig. 2 the experimental methanol (blue) and ethanol (red) isothermal desorption rates versus x_M extracted from the desorption data. For each component, all of the data fall on a nearly linear common curve as expected from an ideal solution.

We have also studied the desorption kinetics using temperature-programmed desorption (TPD) as shown in Fig. 3 (open symbols). The initially layered amorphous binary films were composed of a fixed 30 ML dose of methanol and various amounts of ethanol to yield x_M^0 between 0.85 and 0.15. Again, these results are independent of the initial dosing sequence. Systematic changes in the methanol desorption traces (blue symbols) are observed as x_M^0 decreases. In particular, the desorption peaks shift to higher temperature and the TPD traces broaden significantly. At higher temperatures, ethanol desorption is observed to have a nearly common leading edge reminiscent of zero-order desorption kinetics. Guided by Raoult's law, the methanol desorption rates, dM/dt, are divided by the instantaneous methanol mole fractions, $x_M(t)$, to obtain the temperature-dependent desorption rate for pure liquid methanol, $k_M^o(T)$. This collapses all of the TPD traces onto a single curve (green symbols) which is well fit by an Arrhenius equation (green line). This procedure yields the evaporation rate from pure supercooled liquid methanol that cannot be measured directly because of its rapid crystallization at low temperature (see Fig. 1). We use

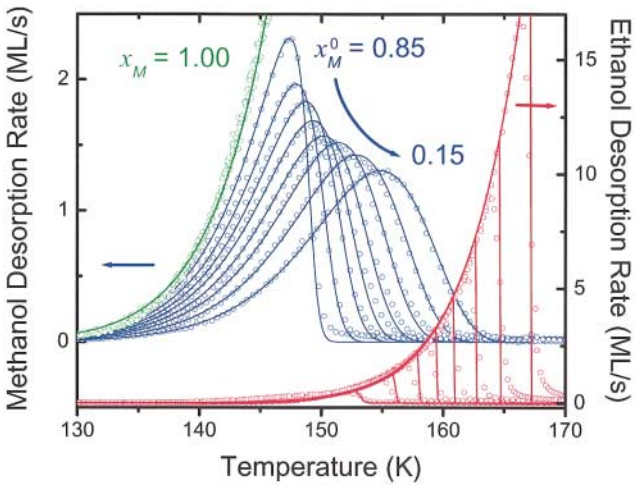

FIG. 3 (color). Methanol (blue) and ethanol (red) TPD (heating rate of 0.6 K/s) for amorphous binary films having initial methanol mole fractions $0.15 \leq x_M^0 \leq 0.85$. (For clarity only every third point is shown.) Ideal solution model simulations are shown as solid lines. The solid green line is an Arrhenius fit to the methanol data normalized by the instantaneous mole fraction (green points) and corresponds to the desorption rate of pure supercooled liquid methanol.

the extracted supercooled methanol desorption parameters [16] to simulate the TPD experiments (solid lines, Fig. 3). The excellent agreement between the simulations and the experimental data indicates that the films continuously mix and obey Raoult's law during their evaporation.

The methanol-ethanol liquid-solid phase diagram [11] is shown in Fig. 4. Superimposed on the phase diagram

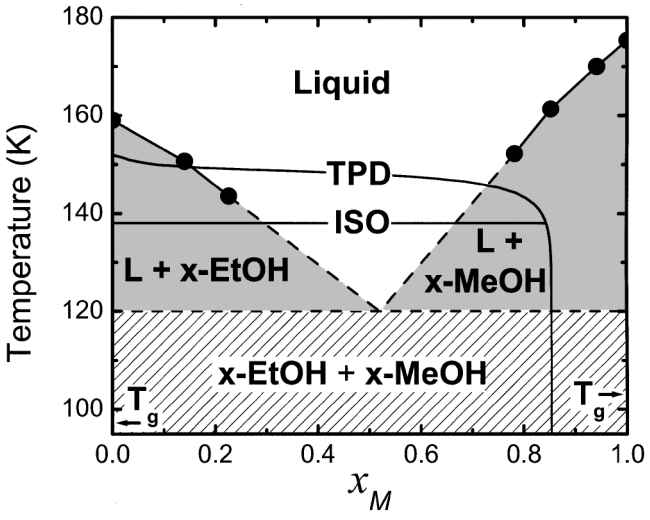

FIG. 4. Methanol-ethanol liquid-solid phase diagram. The solid points are melting point data and the dashed lines correspond to melting and eutectic lines extrapolated from these data [11]. The glass transition temperatures of 103 and 97 K for methanol and ethanol, respectively [8,9], are indicated by the arrows. The solid lines are the trajectories followed by isothermal desorption (ISO) and temperature-programmed desorption (TPD) experiments with $x_M^0 = 0.85$.

are the "trajectories" for isothermal (ISO) and TPD experiments with $x_M^0 = 0.85$. These experiments begin at 20 K and then move vertically at constant x_M as the sample temperature is increased. We observe complete homogeneous intermixing by the onset of measurable desorption at $T \sim 120$ K. Other experiments (not shown here) indicate that the sample does not mix prior to heating above T_g ($\sim$100 K). Since methanol desorbs more rapidly than ethanol, the trajectories start moving toward smaller x_M for $T > 130$ K. The isothermal desorption experiment follows a horizontal line at 138 K while the TPD experiment continues to higher temperatures as methanol evaporates. Similar trajectories can be constructed for the experiments with different x_M^0 but for clarity are omitted here.

The phase diagram shows that the initial intermixing and the subsequent ideal solution evaporation behavior observed in our experiments occur in regions where, at equilibrium, we expect to observe crystallization of one or more of the components. In particular, three distinct phase boundaries are crossed for the trajectories in Fig. 4. However, no evidence of phase transformation is observed upon crossing any of these phase boundaries in either the RAIRS data (Fig. 1) or the desorption data (Figs. 2 and 3). For this to occur, the crystallization time must exceed the experimental desorption time. Although not shown here, we do observe crystallization in experiments employing thicker films that remain in the metastable region longer.

Collectively, these observations indicate that amorphous solid binary films of methanol and ethanol transform into deeply supercooled liquid solutions when heated above their glass transition temperatures ($T_g \sim 100$ K). Furthermore, these thin binary liquid films evaporate as well-mixed ideal solutions, demonstrating that the ideal behavior observed at room temperature [17,18] persists into the deeply supercooled state. These films exhibit liquidlike behavior on the nanoscale while maintaining sufficient macroscopic rigidity to retain their shape—*a beaker without walls.* Compositionally tailored nanoscale amorphous films provide a new means for preparing and examining deeply supercooled solutions in metastable regions of their phase diagram.

This work was supported by the U.S. Department of Energy, Office of Basic Energy Sciences, Chemical Sciences Division. Pacific Northwest National Laboratory is operated for the U.S. Department of Energy by Battelle under Contract No. DE-AC06-76RLO 1830. P. A. gratefully acknowledges support from the National Science and Engineering Research Council of Canada (NSERC).

*Corresponding author.

[1] See *Supercooled Liquids: Advances and Novel Applications,* edited by J. T. Fourkas *et al.* (American Chemical Society, Washington, DC, 1997).
[2] P. G. Debenedetti, *Metastable Liquids: Concepts and Principles* (Princeton University Press, Princeton, NJ, 1996).
[3] R. S. Smith and B. D. Kay, Nature (London) **398**, 788 (1999).
[4] C. A. Angell, Science **267**, 1924 (1995).
[5] K. P. Stevenson *et al.,* Science **283**, 1505 (1999).
[6] R. S. Smith *et al.,* Phys. Rev. Lett. **79**, 909 (1997).
[7] N. Karger, T. Vardag, and H.-D. Lüdemann, J. Chem. Phys. **93**, 3437 (1990).
[8] M. Sugisaki, H. Suga, and S. Seki, Bull. Chem. Soc. Jpn. **41**, 2586 (1968).
[9] O. Haida, H. Suga, and S. Seki, J. Chem. Thermodyn. **9**, 1133 (1977).
[10] G. C. Pimentel and A. L. McClellan, *The Hydrogen Bond* (Freeman, London, 1960), p. 103.
[11] S. Sapgir, Bull. Soc. Chim. Belgium **38**, 392 (1929).
[12] H. Jonsson and H. C. Andersen, Phys. Rev. Lett. **60**, 2295 (1988).
[13] S. R. Williams, I. K. Snook, and W. van Megen, Phys. Rev. E **64**, 021506 (2001).
[14] P. Atkins, *Physical Chemistry* (Freeman, New York, 1994).
[15] R. J. Speedy *et al.,* J. Chem. Phys. **105**, 240 (1996).
[16] The parameters used were $\nu^M = (4.0 \pm 0.5) \times 10^{15}$ ML/s and $E_a^M = 8.8$ kcal/mole for methanol and $\nu^E = (5.5 \pm 0.5) \times 10^{17}$ ML/s and $E_a^E = 12.56$ kcal/mole for ethanol.
[17] J. Timmermans, *The Physico-Chemical Constants of Binary Systems in Concentrated Solutions* (Interscience, New York, 1959).
[18] S.-K. Oh, J. Chem. Eng. Data **42**, 1082 (1997).